Global Journal of Pure and Applied Mathematics.
ISSN 0973-1768 Volume 13, Number 10 (2017), pp. 7009-7033
© Research India Publications
http://www.ripublication.com

# Influence of non-uniform heat source/sink on stagnation point flow of a MHD Casson nanofluid flow over an exponentially stretching surface

**Madasi Krishnaiah[1*], Punnam Rajendar[2*],**
**T. Vijaya Laxmi[2], M. Chenna Krishna Reddy[3]**

*[1*,2*,2,3]Department Of Mathematics, Osmania University,*
*Hyderabad, Telangana, India.*
*[2]NTR .Govt. Degree College (W), Mahabubnagar-509001,*
*Telangana, India.*

**Abstract**

This paper deals with the influence of non uniform heat source on stagnation point flow of a MHD casson nanofluids over an exponentially stretching sheet with heat and mass transfer. Casson fluid model is used to characterize the non-Newtonian fluid behaviour. Using suitable similarity transformations, the governing boundary-layer equations corresponding to the momentum, energy and concentration are reduced to a set of self-similar non-linear ordinary differential equation. The transformed equations are then solved numerically using Keller Box method. Effects of various physical parameters are displayed graphically for velocity, temperature and concentration profiles. Also the behaviour of skin friction coefficient, Nusselt number and Sherwood number are presented through tabular.

**Keywords:** Exponentially stretching surface, casson nanofluid, stagnation point, MHD, non uniform heat source/sink.

## INTRODUCTION

The fluid flow behaviour of non-Newtonian fluid has attracted special interest in recent years due to the wide application of these fluids in the chemical, pharmaceutical, petrochemical, food industries and electronic industries. Fluids that belong to this category include cement, drilling mud, sludge, granular suspensions, acquires foams, slurries, paints, plastics, paper pulp and food products. Many fluids that are used extensively in industrial application are non-Newtonian fluids exhibiting a yield stress $\tau_y$, stress that has to be exceeded before the fluid moves. As a result the fluid cannot sustain a velocity gradient unless the magnitude of the local shear stress is higher than this yield stress. Due to the increasing importance of non-Newtonian fluids in industry, the stretching sheet concept has more recently been extended to fluids obeying non-Newtonian constitutive equations (Prasad et al. [1]).

Stagnation point flow is continuing to be an interesting area of research among scientists and investigators due to its importance in a wide variety of applications both in industrial and scientific applications. Many researchers have been working still on the stagnation- point flow in various ways. Accordingly, Mahapatra and Gupta [2] numerically analyzed two dimensional boundary layer flow, stagnation point flow and heat transfer over a stretching sheet. Their result indicated that a boundary layer is formed when the stretching velocity is less than a free stream velocity and an inverted boundary layer is formed when the stretching velocity exceeds the free steam velocity. By considering a special case of stretching sheet, Wang [3] studied two dimensional stagnation point flow on a two dimensional shrinking sheet and axisymmetric stagnation point flow on an axisymmetric shrinking sheet. In all the above studies the investigators considered the stagnation point flow when the line of stagnation is perpendicular to the stretching surface. But Sometimes there might be a situation were an oblique line stagnation point is important. It was found that the obliqueness of a free stream line causes the shifting of the stagnation point towards the incoming flow.

Nazar et al. [4] was studied in non-Newtonian fluids, the stagnation point flow of a micropolar fluid towards a stretching sheet. Similarly Ishak et al. [5] investigated stagnation-point flow over a shrinking sheet in a micropolar fluid. Their results indicated that the solution is different from a stretching sheet, and it was found that the solutions for a shrinking sheet are not unique. Furthermore, Ishak et al. [6] numerically analyzed a mixed stagnation point flow of a micropolar fluid towards a stretching sheet. They point out that micropolar fluid showed more drag reduction characteristic when compared to classical Newtonian fluid. Similarly, Hayat et al. [7] discussed the MHD flow of a micropolar fluid near a stagnation point towards a non-

linear stretching surface. Further, Nadeem et al. [8] extended the problem to porous medium and investigated MHD stagnation flow of a micropolar fluid through a porous medium. Also, Ashraf [9] incorporated the heat transfer parameter to stagnation point flow and studied MHD stagnation point flow of a micropolar fluid towards a heated vertical surface. Ali et al. [10] included the idea of induced magnetic field to the problem of Ashraf and analyzed MHD stagnation-point flow and heat transfer towards stretching sheet with induced magnetic field. Moreover, Hayat et al. [11] investigated stagnation-point flow of a Maxwell fluid with magnetic field and radiation effect. They discussed the effects of heat transfer on a steady two-dimensional stagnation point flow of a Maxwell fluid over a stretching sheet.Pramaik [12] investigated the Casson fluid flow of an exponentially porous stretching surface in the presence of thermal radiation. Mukhopadyay [13] investigated the MHD boundary layer flow of an exponential stretching sheet embedded in a thermally stratified medium and also conclude that fluid velocity and temperature decreases significantly with increasing suction parameter.

The study of the magnetohydrodynamic (MHD) flow of an electrically conducting fluid due to a stretching sheet is important in modern metallurgy and metal-working processes. The process of fusing of metals in an electrical furnace by applying a magnetic field and the process of cooling of the first wall inside a nuclear reactor containment vessel where the hot plasma is isolated from the wall by applying a magnetic field are some examples of such fields. Boundary-layer and Magnetohydrodynamics stagnation point flow towards a stretching sheet studied numerically by Mahapatra and Gupta [14] and Ishak [15]. Their analysis showed that velocity at a point increase with an increase in the magnetic field when the free stream velocity is greater than the stretching velocity. Mahapatra et al. [16] extend their investigation to a power-law fluid and studied the magnetohydrodynamic stagnation point flow of a power-law fluid towards a stretching surface. The result signifies that for a given magnetic parameter, the dimensionless shear stress coefficient increases in magnitude with an increase in power-law index when the values of the ratio of free stream velocity and stretching velocity are close to 1. Furthermore, Ishak et al. [17] studied MHD mixed convection flow near the stagnation- point on a vertical permeable surface. Gangadhar [18] studied the heat and mass transfer over a vertical plate with a convective surface boundary condition and chemical reaction and also conclude that the spices boundary layer thickness decreases with increasing the chemical reaction parameter. Abel et al.[19] and Bataller analysed the effects of non-uniform heat source on viscoelastic fluid flow and heat transfer over a stretching sheets. Sandeep et al. [20] studied the impact of

non uniform heat source/sink on dusty nanofluid flow past a stretching/shrinking sheet. In most of these investigations, the flow and temperature fields were considered at steady state. Recently, Sandeep et al. [21] discussed the influence of non uniform heat source/sink on the flow of dusty nanofluid past a stretching /shrinking cylinder. Similar type of study past a slendering stretching sheet was reported by Ramana Reddy et al. [22].

The present study investigates the numerical solutions for a class of nonlinear differential equations arising in heat and mass transfer of a non-Newtonian fluid towards an exponentially stretching surface is obtained. Casson fluid model is used to characterize the non-Newtonian fluid behaviour.

## FORMULATION OF THE PROBLEM:

Consider the flow of an incompressible viscous fluid past a flat sheet coinciding with the plane $y = 0$. The fluid flow is confined to $y > 0$. Two equal and opposite forces are applied along the $x$-axis so that the wall is stretched keeping the origin fixed and this two-dimensional stagnation point flow of a nanofluid towards a stretching sheet kept at a constant temperature $T_w$ and concentration $C_w$. The ambient temperature and concentration respectively are $T_\infty$ and $C_\infty$. The flow is subjected to a constant transverse magnetic field of strength $B = B_0$ which is assumed to be applied in the positive y-direction, normal to the surface. The induced magnetic field is assumed to be small compared to the applied magnetic field and is neglected. It is further assumed that the base fluid and the suspended nanoparticles are in thermal equilibrium and no slip occurs between them. In addition, we considered the effects non-uniform heat source/sink.

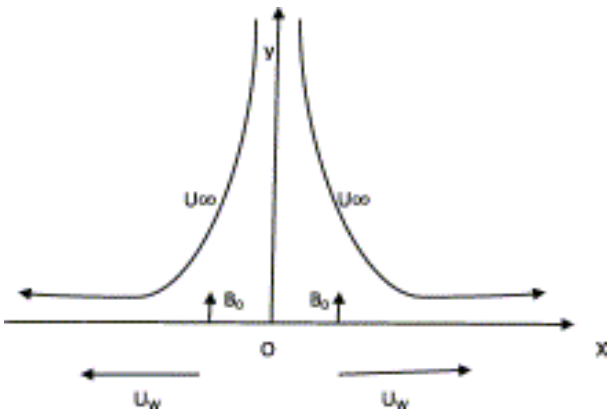


**Figure 1.** Flow configuration and coordinate system.

The physical flow model and coordinate system is shown in Fig 1. Under boundary layer approximations, the flow and heat transfer with the effects non-uniform heat source/sink are governed by the following dimensional form of equations.

$$\frac{\partial u}{\partial x}+\frac{\partial v}{\partial y}=0 \tag{1}$$

$$u\frac{\partial u}{\partial x}+v\frac{\partial u}{\partial y}=\nu\left(1+\frac{1}{\beta}\right)\frac{\partial^2 u}{\partial y^2}-\frac{\sigma B^2}{\rho}u+U_\infty\frac{\partial U_\infty}{\partial x}+\frac{\sigma B_0^2}{\rho_f}U_\infty \tag{2}$$

$$u\frac{\partial T}{\partial x}+v\frac{\partial T}{\partial y}=\alpha\frac{\partial^2 T}{\partial T^2}-\frac{1}{\rho c_p}q'''+\tau\left(D_B\left(\frac{\partial C}{\partial y}\frac{\partial T}{\partial y}\right)+\frac{D_T}{T_\infty}\left(\frac{\partial T}{\partial y}\right)^2\right) \tag{3}$$

$$u\frac{\partial C}{\partial x}+v\frac{\partial C}{\partial y}=D_B\frac{\partial^2 C}{\partial y^2}+\frac{D_T}{D_\infty}\frac{\partial^2 T}{\partial y^2}-k\left(C-C_\infty\right) \tag{4}$$

where $u$ and $v$ are the components of the velocity in the $x$ and $y$ directions respectively, $\nu$ is the kinematic viscosity, $\alpha$ is thermal diffusivity, $T$ is the fluid temperature in the boundary layer, $\rho$ is fluid density, $C_p$ is the specific heat at constant pressure.

The boundary conditions are

$$u=U_w(x)=ae^{\frac{x}{L}},\quad v=v_w(x),T=T_w,C=C_w\quad at\quad y=0 \tag{7}$$

$$u\to 0,T\to T_\infty,C\to C_\infty\quad as\quad y\to\infty \tag{8}$$

Where $V_w(x)=V_0e^{\frac{x}{L}}$, $U_\infty=be^{\frac{x}{L}}$ *and* $q'''=\frac{ku_w(x)}{l\nu}\left[A^*(T_w-T_\infty)f'(\eta)+B^*(T-T_\infty)\right]$

Where $T_w$ is the variable temperature at the sheet with $T_0$ being a constant and $C_w$ is the variable concentration at the sheet with $C_0$ being constant. It is assumed that the

magnetic field *B(x)* is of the form $B(x) = B_0 e^{\frac{x}{2L}}$ where $B_0$ is a constant magnetic field.

The continuity equation (1) is satisfied by introducing a stream function $\psi$ such that

$$u = \frac{\partial \psi}{\partial y} \quad and \quad v = -\frac{\partial \psi}{\partial x}$$

For non dimensionalized form of momentum and energy equations as well as boundary conditions, the following transformations are introduced.

$$\eta = y\sqrt{\frac{a}{2\nu L}} e^{\frac{x}{2L}},\ u = ae^{\frac{x}{L}} f'(\eta),\quad v = -\sqrt{\frac{\nu a}{2L}} e^{\frac{x}{2L}} \left( f(\eta) + \eta f'(\eta) \right)$$

$$T = T_\infty + T_0 e^{\frac{x}{2L}} \theta(\eta) \quad and \quad C = C_\infty + C_0 e^{\frac{x}{2L}} \phi(\eta) \tag{11}$$

Where $\eta$ is the similarity variable, $f(\eta)$ is the dimensionless stream function, $\theta(\eta)$ is the dimensionless temperature, $\phi(\eta)$ is the dimensionless concentration and prime denote differentiation with respect to $\eta$. Using the similarity transformations, the governing equations have been transformed into a system of ordinary differential equations. The momentum, energy and concentration equations can be reduced into ordinary differential equations

$$\left(1 + \frac{1}{\beta}\right) f''' + ff'' - 2(f')^2 + M(A - f') + 2A^2 = 0 \tag{12}$$

$$\theta'' + P_r f\theta' - P_r f'\theta - A^* f' - B^*\theta + P_r Nb\phi'\theta' + P_r Nt(\theta')^2 = 0 \tag{13}$$

$$\phi'' + S_c \left( f\phi' - f'\phi - 2k_r\phi \right) + \frac{Nt}{Nb}\theta'' = 0 \tag{14}$$

The transformed boundary conditions of the problem are

$$f(0) = f_w,\ f'(0) = 1, \theta(0) = 1, \phi(0) = 1,\ f'(\infty) = A, \theta(\infty) = 0, \phi(\infty) = 0 \tag{15}$$

Where $f'$ is the dimensionless velocity, $\theta$ is the temperature, $\phi$ is the particle on centration, $M = \frac{2\sigma B_0^2 L}{a\rho}$ is the magnetic parameter , $A = \frac{b}{a}$ is velocity ratio, $P_r = \frac{\nu}{\alpha}$ is the prandtlnumber, $S_c = \frac{\nu}{D}$ is the Schmidtnumber, $Nb = \frac{\rho c_p D_B(\phi_w - \phi_\infty)}{\rho c_f \nu}$ is the

Brownian motion parameter, $Nt = \frac{\rho c_p D_T (T_w - T_\infty)}{\rho c_f \nu T_\infty}$ is the thermoporesisparameter, $f_w = -\frac{V_0}{\sqrt{\frac{a\nu}{2L}}}$ is the wall mass flux parameter and $k_r = \frac{k_0 L}{a}$ is the reaction rate parameter here $k_r>0$, $\beta$ is the casson fluid parameter.

**NUMERICAL METHOD**:

The higher order ordinary differential equations with the boundary conditions are solved numerically by using implicit finite difference scheme known as Keller-Box method, the following steps are involved to achieve the Numerical solution.

Reduce the non-linear higher order ordinary differential equations into a system of first order ordinary differential equations. Write the finite differences for the first order equations. Linearize the algebraic equations by Newton's method, and write them in matrix–vector form. Solving the linear system by the block tri-diagonal elimination technique.

In order to solve the above differential equations numerically, we adopt Mat lab software which is very efficient in using the well known Keller box method.

For getting accuracy of this method to choose appropriate initial guesses.

$$f(\eta) = 1 - \frac{v_0}{\sqrt{\frac{a\nu}{2L}}} - e^{-\eta}, \quad \theta(\eta) = e^{-\eta}, \quad \phi(\eta) = e^{-\eta}$$

The step size $\delta = 0.01$ is used to obtain numerical solution with four decimal place accuracy as criterion of convergence.

**RESULT AND DISCUSSION:**

The theme of this section is to discuss the effect of various physical parameters such as Magnetic parameter M, Velocity ratio A, Prandtl number Pr, Reaction rate parameter Kr, Brownian motion parameter Nb, Themoporesis parameter Nt, Lewis number Le, Wall mass flux parameter $f_w$, schmidt number Sc, Space dependent parameter $A^*$ and temperature dependent parameter $B^*$.

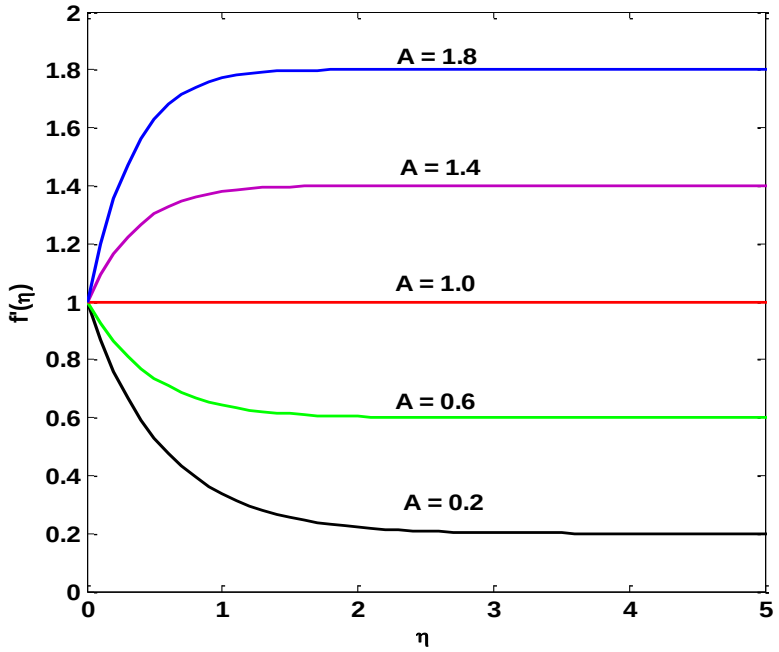


**Figure 2.** Effect of velocity ratio parameter A on velocity profile

Fig. 2 illustrates the influence of velocity ratio parameter A on velocity graph. When the free stream velocity exceeds the velocity of the stretching sheet, the flow velocity increases and the boundary layer thickness decreases with increase in A. Moreover, when the free stream velocity less than stretching velocity, the flow field velocity decreases and boundary layer thickness also deceases. When A> 1, the flow has a boundary layer structure and boundary layer thickness decreases as values of A increases. On the other hand, when A< 1, the flow has an inverted boundary layer structure, for this case also, as the values A decrease the boundary layer thickness decreases.

Fig. 3 shows the variation of temperature profile in response to a change in the values of velocity ratio parameter A. It shows that as velocity ratio parameter increases the thermal boundary layer thickness decreases. Moreover, the temperature gradient at the surface increase (in absolute value) as A increases. As a result, temperature profile decreases.

Fig. 4 shows the variation of concentration profile in response to a change in the values of velocity ratio parameter A. It shows that as velocity ratio parameter increases the thermal boundary layer thickness decreases. Moreover, the

concentration gradient at the surface increases as A increases. As a result, concentration profile decreases.

In the Fig. 5, 6 and 7 the magnetic parameter M represents the importance of magnetic field on the flow field, temperature and concentration. The presence of transverse magnetic field sets in Lorentz force, which results in retarding force on the velocity field. Therefore, as the values of M increase, so does the retarding force and hence the velocity decreases where as temperature and concentration profiles increases.

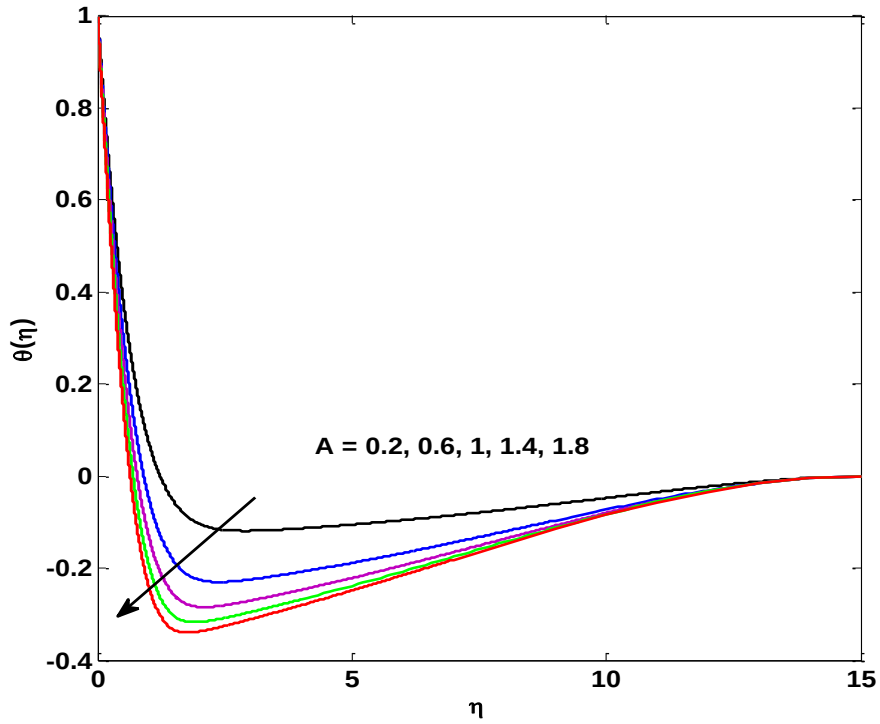


**Figure 3.** Effect of velocity ratio parameter A on temperature profile

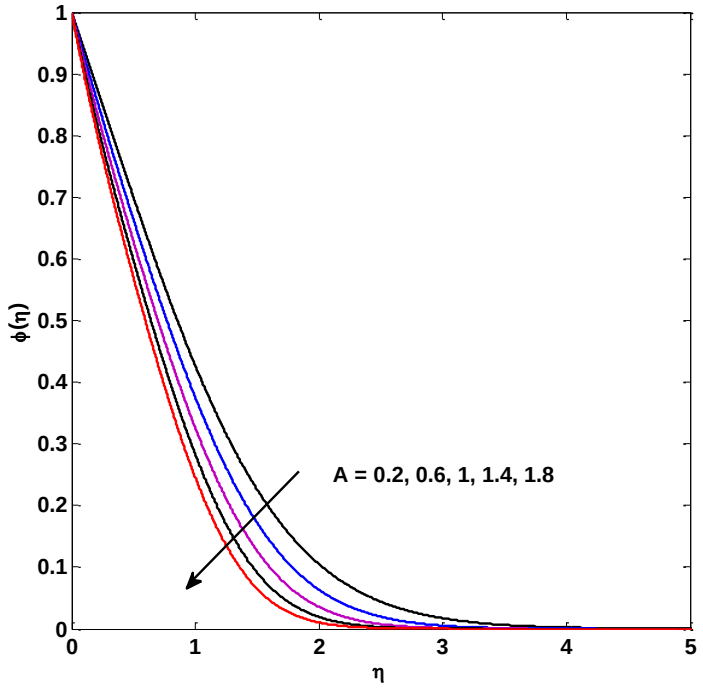


**Figure 4.** Effect of velocity ratio parameter A on concentration profile

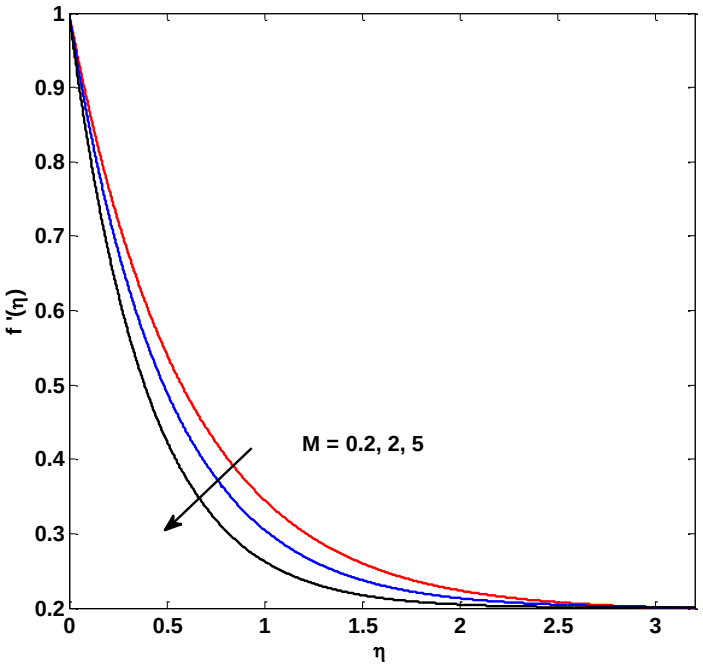


**Figure 5.** Effect of magnetic parameter M on velocity profile

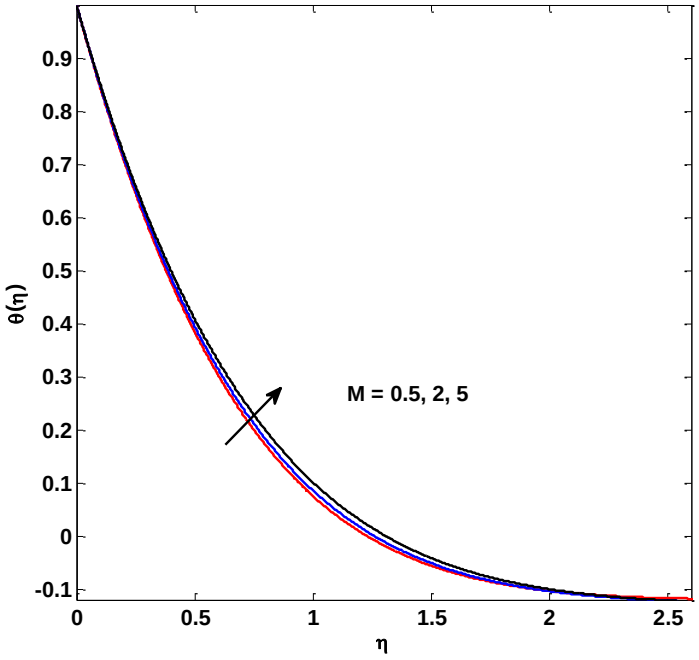


**Figure 6.** Effect of magnetic parameter M on temperature profile

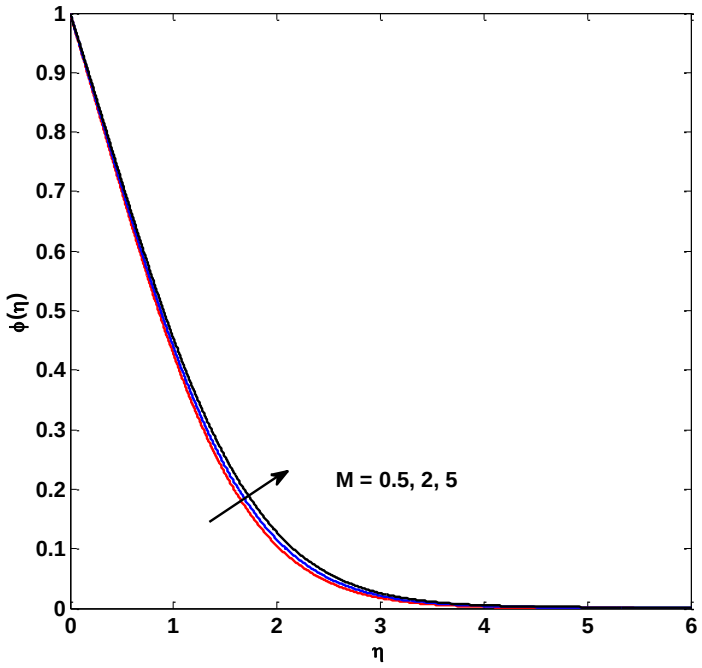


**Figure 7.** Effect of magnetic parameter M on concentration profile.

Figs. 8, 9 and 10 present the response of velocity (Fig. 8), temperature (Fig. 9) and concentration profiles (Fig.10) for a variation in Casson fluid parameter. Temperature of the fluid increases throughout the boundary layer with an increasing in the Casson parameter and consequently thermal boundary layer thickness enhanced and opposite results were found with an rising temperature and concentration profiles and decreases in velocity.

Figs. 11, 12 and 13 present the response of velocity (Fig. 11), temperature (Fig. 12) and concentration profiles (Fig. 13) for a variation in Wall mass flux parameter $f_w$. Temperature of the fluid decreases throughout the boundary layer with an increasing in the wall mass flux parameter and consequently thermal boundary layer thickness decreases obviously results were found with decreases in velocity, temperature and concentration profiles.

From fig.14 it is found that as Pr increases, the temperature in the boundary layer decreases and the thermal boundary layer thickness also decreases. This is because for small values of the Prandtl number, the fluid is highly thermal conductive. Physically, if Pr increases, the thermal diffusivity decreases and these phenomena lead to the decreasing of energy ability that reduces the thermal boundary layer.

The temperature profiles for different space-dependent and temperature-dependent parameters for heat source/sink are presented in Figures 15 and 16, respectively. It is observed that both $A^*$ and $B^*$ increases the temperature profiles. The heat generation source ($A^* > 0$ and $B^* < 0$) leads to a larger thermal diffusion boundary layer that may increase the thermal boundary layer thickness; on the contrary, the layer thickness decreases for heat absorption sink ($A^* < 0$ *and* $B^* > 0$).

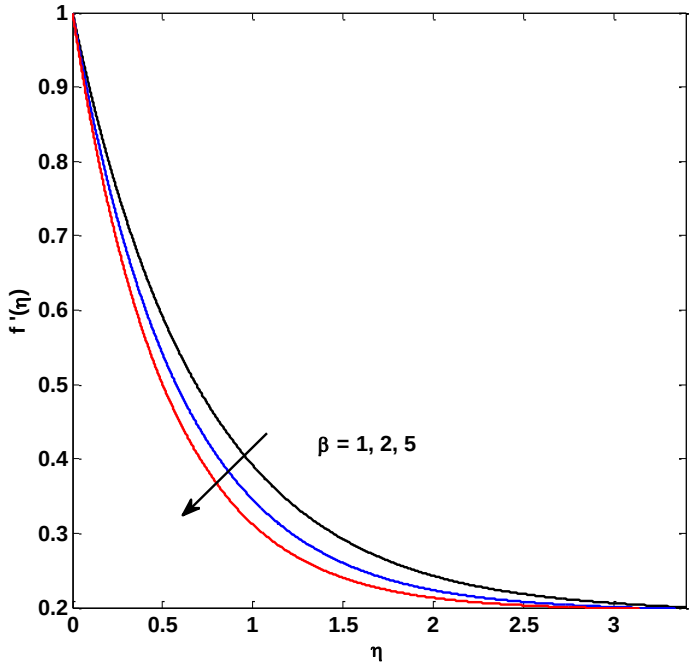


**Figure 8.** Effect of Casson fluid parameter $\beta$ on velocity profile

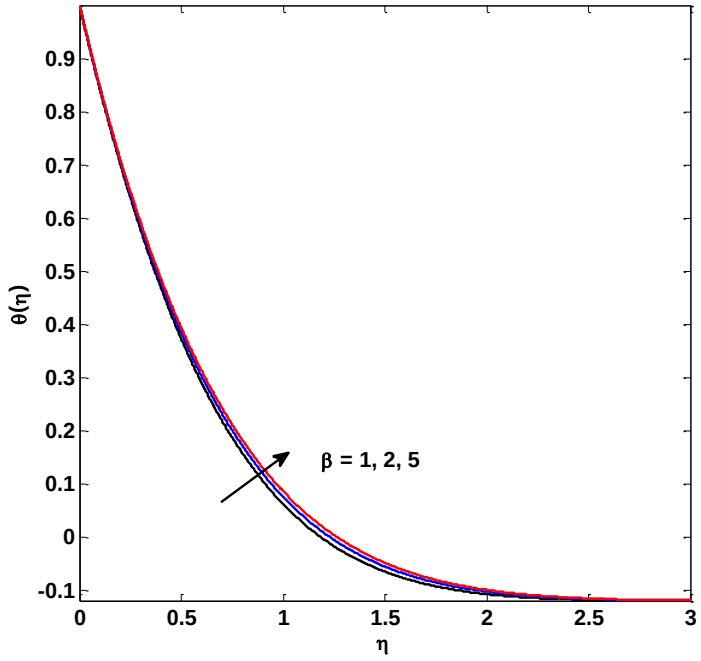


**Figure 9.** Effect of Casson fluid parameter $\beta$ on temperature profile

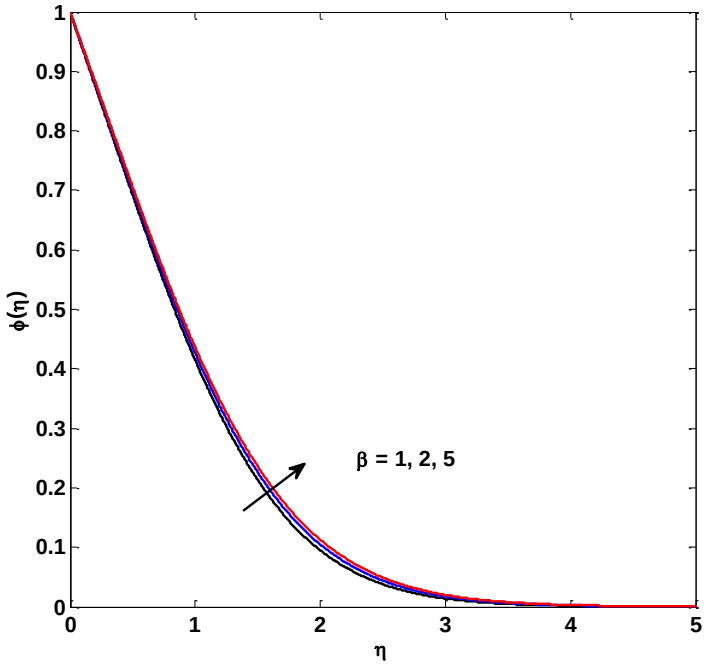


**Figure 10.** Effect of Casson fluid parameter $\beta$ on concentration profile

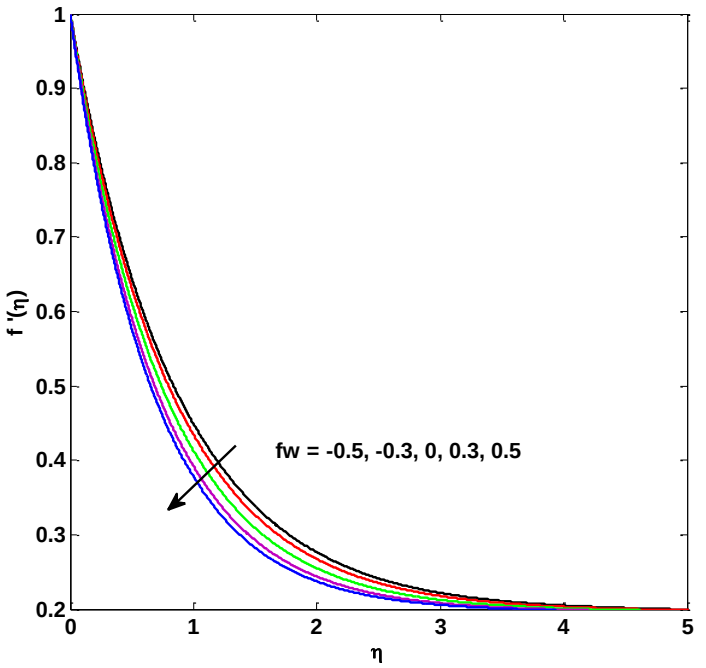


**Figure 11.** Effect of wall mass flux parameter $f_w$ on velocity profile

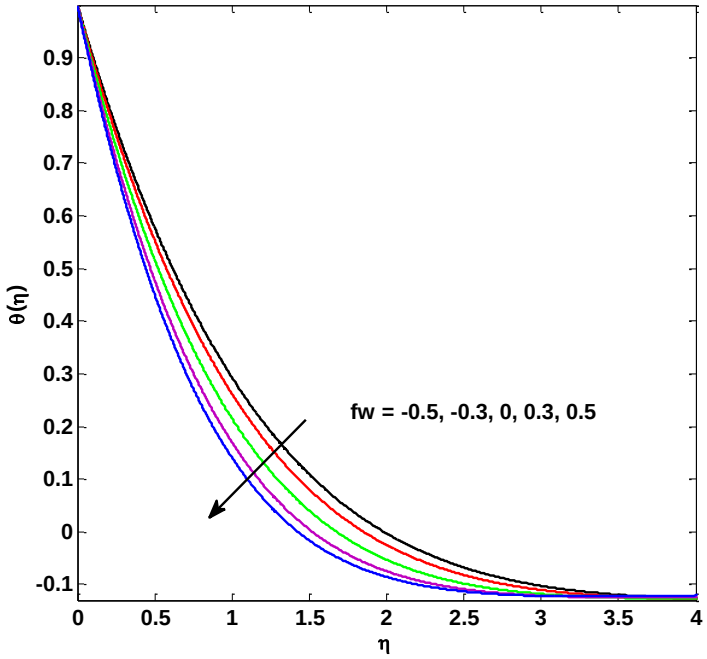


**Figure 12.** Effect of wall mass flux parameter $f_w$ on temperature profile

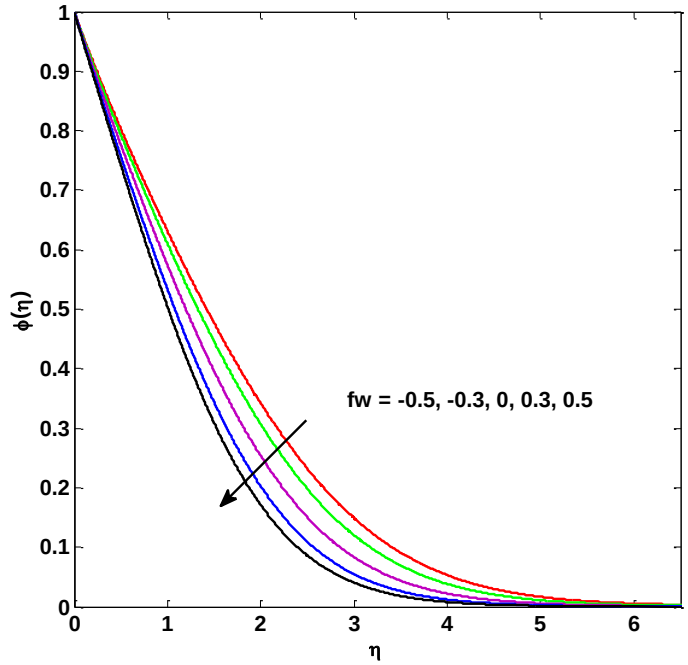


**Figure 13.** Effect of wall mass flux parameter $f_w$ on concentration profile

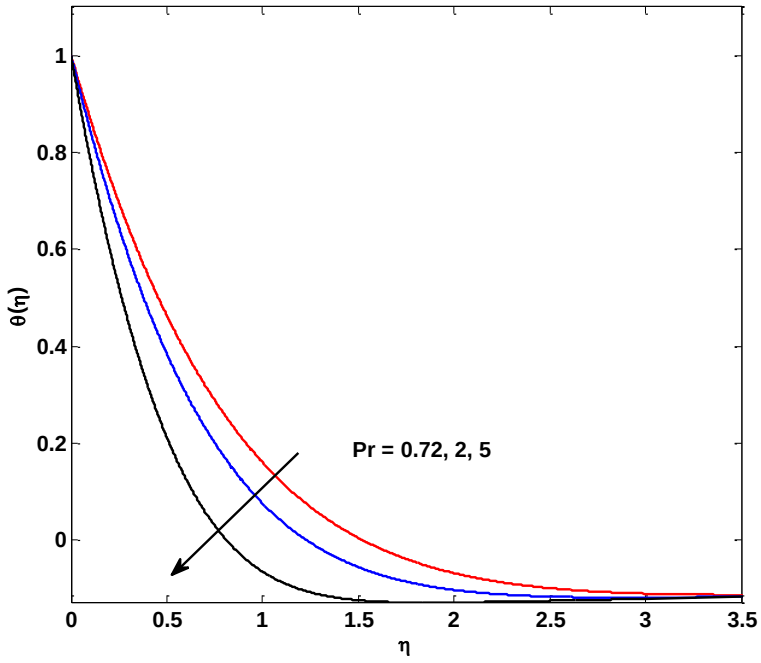


**Figure 14.** Effect of Prandtl number Pr on temperature profile

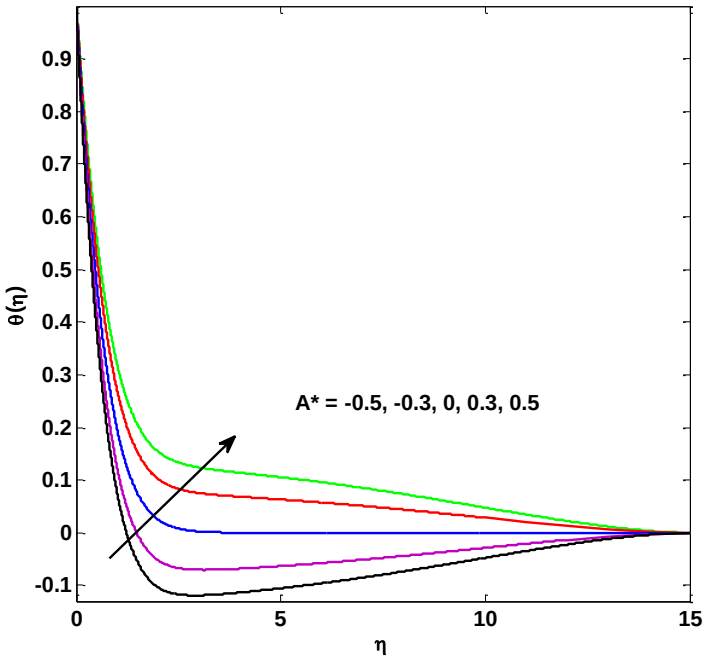


**Figure 15.** Effect of space dependent parameter $A^*$ on temperature profile

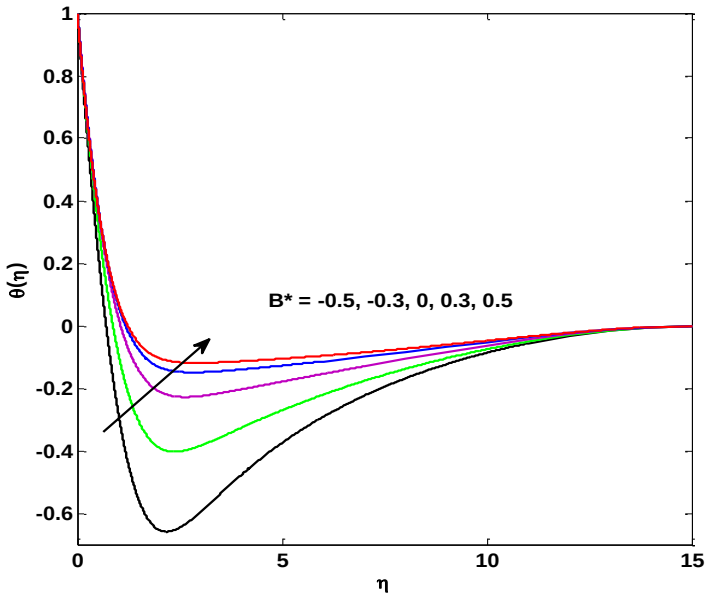


**Figure 16.** Effect of temperature dependent parameter $B^*$ on temperature profile.

Fig.17 and 18 reveals variation of temperature and concentration graph in response to a change in Brownian motion parameter Nb. The influence of Brownian motion on temperature, concentration profile graph is as the values of Brownian motion parameter increase, the concentration boundary layer thickness is decreasing and temperature increases. The graph also reveals that the thermal boundary layer thickness does not change much when the values of Nb increases.

Fig.19 and 20 reveals variation of Temperature and concentration graph in response to a change in thermoporesis parameter Nt. The influence of thermoporesis on temperature and concentration profile graph is as the values of thermoporesis parameter increases. The graph also reveals that the thermal boundary layer thickness change much when the values of Nt increases.

In Figures 21 and 22 the concentration boundary layers are observed to decreases with increasing values of the Reaction rate parameter and the Schmidt number.

Table-1 shows comparison for the values of local Nussult number for various values of Pr.

We observed that, which are very closely agree to the previous published data.

Table-2 depicts that computed of skin friction coefficient for various dimensionless parameters $A$, $M$, $\beta$, $f_w$.

Table-3 shows the effects of varying various controlling parameters on the rate of heat and mass transfers at the sheet surface. It is observed that both the rate of heat and the mass transfer increase with the increase of Prandtl (*Pr*) numbers. A similar observation was made, the rate of heat transfer for the space-dependent (*A**) and temperature-dependent (*B**) parameters but decreases in the rate of mass transfer.

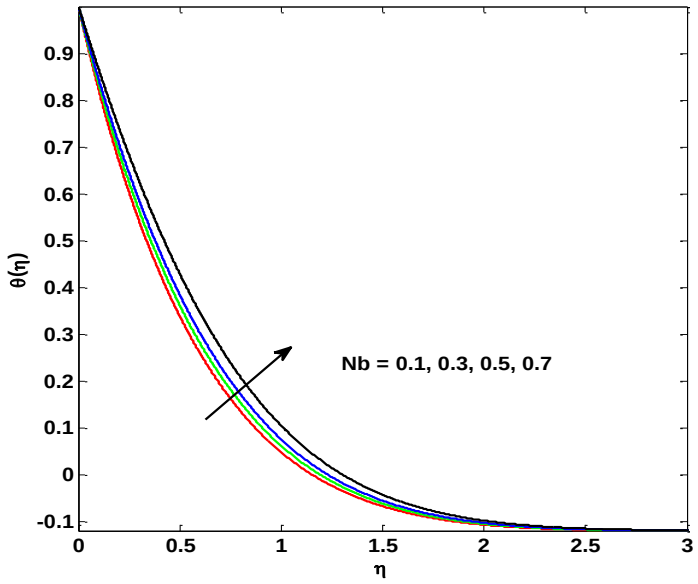


**Figure 17.** Effect of Brownian motion parameter Nb on temperature profile

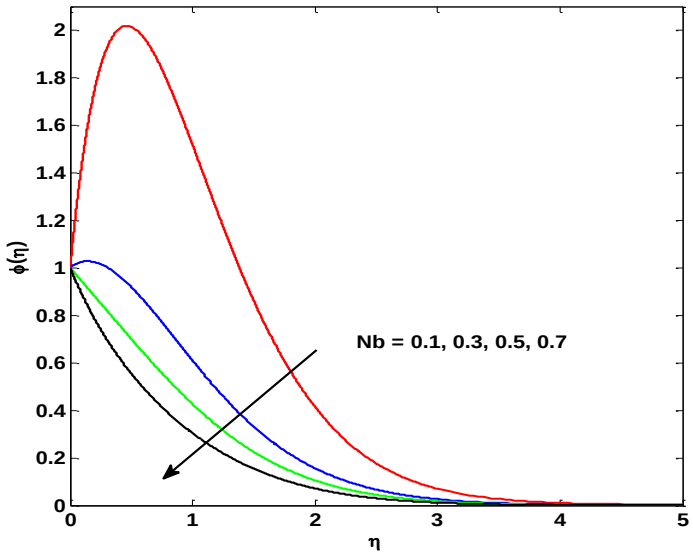


**Figure 18.** Effect of Brownian motion parameter Nb on concentration profile

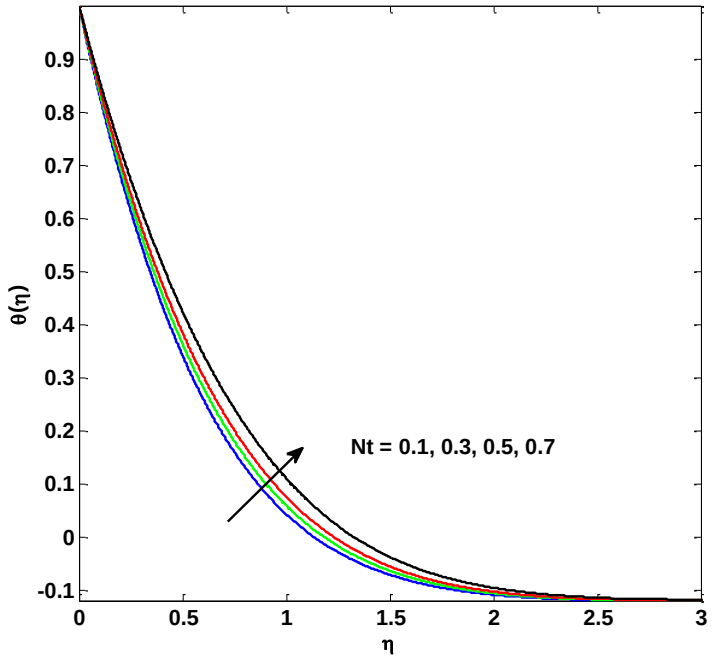


**Figure 19.** Effect of thermoporesis parameter Nt on temperature profile

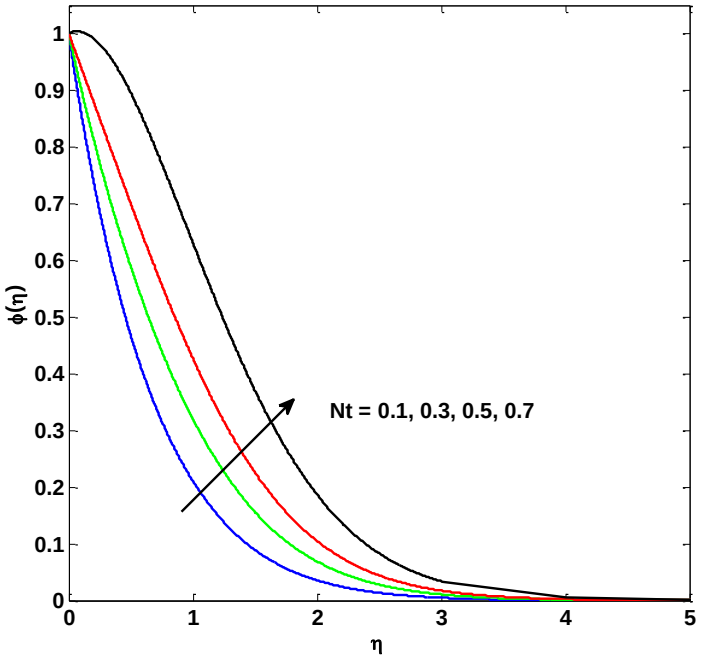


**Figure 20.** Effect of thermoporesis parameter Nt on concentration profile

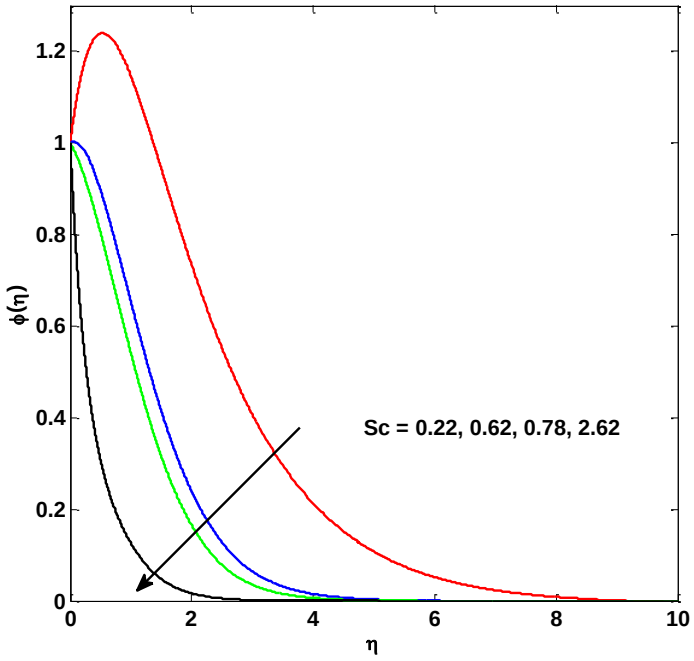


**Figure 21.** Effect of schmidt number Sc on concentration profile

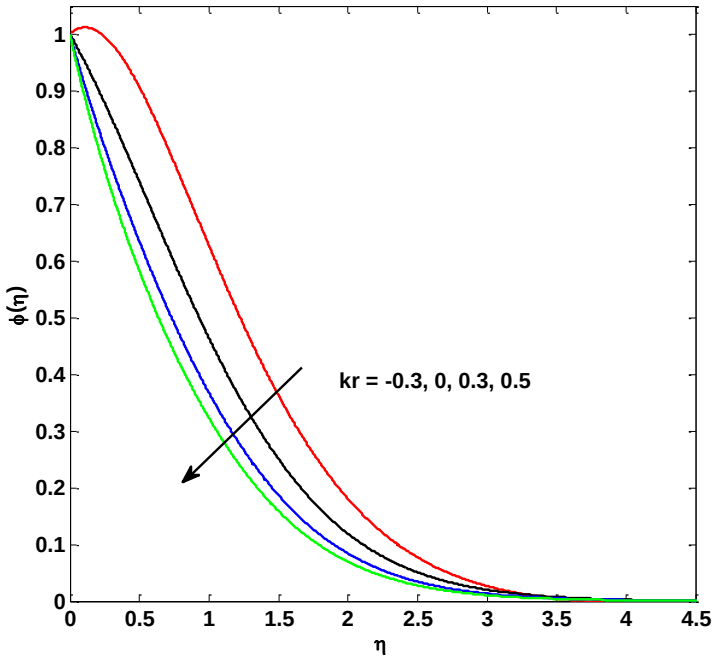


**Figure 22.** Effect of reaction rate parameter Kr on concentration profile

**Table 1.** Comparison for the values of $-\theta'(0)$ for various values of Pr

| Pr | El Aziz [23] | Sharma *et al* [24] | Prasannakumar et al [25] | Present Result |
|---|---|---|---|---|
| 1.0 | 0.9547 | 0.9547 | 0.9548 | 0.9548 |
| 2.0 | -------- | 1.4714 | 1.4714 | 1.4715 |
| 3.0 | 1.8690 | 1.8690 | 1.8690 | 1.8691 |
| 5.0 | 2.5001 | 2.5001 | 2.5001 | 2.5001 |
| 10.0 | 3.6603 | 3.6603 | 3.6603 | 3.6604 |

**Table 2.** Calculation of skin friction coefficient for various values $A, M, \beta, f_w$.

| A | M | $\beta$ | $f_w$ | $-f''(0)$ |
|---|---|---|---|---|
| 0.5 | 1.0 | 2.0 | 1.0 | 1.0136 |
| 0.2 | | | | 1.4697 |
| 0.3 | | | | 1.3324 |
| 0.6 | | | | 0.8343 |
| | 2.0 | | | 1.1.54 |
| | 3.0 | | | 1.1898 |
| | 4.0 | | | 1.3411 |
| | | 3.0 | | 1.0879 |
| | | 4.0 | | 1.1313 |
| | | 5.0 | | 1.1597 |
| | | | 0.1 | 0.8434 |
| | | | 0.5 | 0.9156 |
| | | | 1.5 | 1.1199 |

**Table 3.** Calculation of Nusselt number and Sherwood number for various values Pr, Nb, Nt, $A^*$, $B^*$, $K_r$, Sc.

| Pr | Nb | Nt | $A^*$ | $B^*$ | $K_r$ | Sc | $-\theta'(0)$ | $-\phi'(0)$ |
|---|---|---|---|---|---|---|---|---|
| 1.0 | 0.1 | 0.1 | 0.5 | 0.5 | 0.2 | 1.0 | 2.2275 | 1.0840 |
| 2.0 | | | | | | | 3.5297 | 0.1306 |
| 5.0 | | | | | | | 6.6877 | 3.1868 |
| | 0.5 | | | | | | 1.7174 | 2.5161 |
| | 1.0 | | | | | | 1.2299 | 2.6803 |
| | 1.5 | | | | | | 0.8818 | 2.7260 |
| | | 0.2 | | | | | 2.1677 | 0.4764 |
| | | 0.3 | | | | | 2.1101 | 1.9336 |
| | | 0.5 | | | | | 2.0014 | 4.5636 |
| | | | 0.2 | | | | 0.7706 | 2.7304 |
| | | | 0.4 | | | | 0.8448 | 2.7274 |
| | | | 0.6 | | | | 0.9188 | 2.7245 |
| | | | | 0.2 | | | 0.8209 | 2.7302 |
| | | | | 0.4 | | | 0.8613 | 2.7274 |
| | | | | 0.6 | | | 0.9025 | 2.7246 |
| | | | | | 0.0 | | 2.2796 | 0.0475 |
| | | | | | 0.5 | | 2.1513 | 2.6369 |
| | | | | | 1.0 | | 2.0291 | 6.0909 |
| | | | | | | 0.3 | 1.4057 | 1.0820 |
| | | | | | | 0.5 | 1.1757 | 1.6049 |
| | | | | | | 0.7 | 1.0280 | 2.0749 |

## CONCLUSIONS:

In the present prate, Influence of Non uniform heat source/sink on a stagnation point flow of a MHD Casson nanofluid flow over an exponentially stretching surface was analysed. Casson fluid model is used to characterize the non-Newtonian fluid behaviour. Numerical calculations are carried out for various values of the dimensionless parameters of the problem. It has been found that

- Momentum boundary layer thickness and temperature increases with increasing Cassonfluid parameter but the velocity decreases in this case.
- Velocity and Temperature as well as boundary layer thickness reduces with the influence of wall mass flux parameter $f_w$.
- Thermal boundary layer thickness decreases with a rising the Prandtl number. As a result temperature decreases.
- With increasing Sc and Kr, concentration decreases for increase in Schmidt number and reaction rate parameter which reduces the boundary layer thickness.
- It was observed that temperature rising with the increasing of space-dependent (A*) and temperature dependent (B*) parameters for heat source/sink.

## REFERENCES

[1] Prasad, K. V., Abel, S., &Datti, P. S., Diffusion of chemically reactive species of a non- Newtonian fluid immersed in a porous medium over a stretching sheet, Int. J. of Non-Linear Mech., Vol.38, pp. (2003)651 – 657.

[2] T.R. Mahapatra, A.G. Gupta, Heat transfer in stagnation point flow towards a stretchingsheet, Heat Mass Transfer 38 (2002) 517–521.

[3] C.Y. Wang, Stagnation point flow towards a shrinking sheet, Int. J. Non-Linear Mech. 43 (2008) 377–382.

[4] R. Nazar, N. Amine, D. Filip, I. Pop, Stagnation point flow of a microploar fluid towards a stretching sheet, Int. J. Non-Linear Mech. 39 (2004) 1227–1235.

[5] A. Ishak, Y.Y. Lok, I. Pop, Stagnation-point flow over a shrinking sheet in a micropolar fluid, Chem. Eng. Commun. 197 (2010) 1417–1427.

[6] A. Ishak, R. Nazar, I. Pop, Mixed convection stagnation point flow of a

micropolar fluid towards a stretching sheet, Mechanica 43 (2008) 411–418.

[7] T. Hayat, T. Javed, Z. Abbas, MHD flow of a micropolar fluid near a stagnationpoint towards a non-linear stretching surface, Non-Linear Analysis: Real World Applications 10 (2009) 1514–1526.

[8] S. Nadeem, M. Hussani, M. Naz, MHD stagnation flow of a micropolar fluid through a porous medium, Mechanica 45 (2010) 869–880.

[9] M. Ashraf, M.M. Ashraf, MHD stagnation point flow of a micropolar fluid towards a heated surface, Appl. Math. Mech. -Engl. Ed. 32 (1) (2011) 45–54.

[10] F.M. Ali, R. Nazar, N.M. Arifin, I. Pop, MHD stagnation-point flow and heat transfer towards stretching sheet with induced magnetic field, Appl. Math. Mech. -Engl. Ed. 32 (4) (2011) 409–418.

[11] T. Hayat, A. Rafique, M.Y. Malik, S. Obaidat, Stagnation-point flow of Maxwell fluid with magnetic field and radiation effects, Heat Transfer – Asian Research 41 (1) (2012) 23–32.

[12] Pramanik, S., Casson fluid flow and heat transfer past an exponentially porous stretching surface in presence of thermal radiation, Ain Shams Engineering Journal, Vol.5, pp. (2014)205–212.

[13] Swati Mukhopadhyay, MHD boundary layer flow and heat transfer over an exponentially stretching sheet embedded in a thermally stratified medium, Alexandria Engineering Journal, Vol.52, pp. (2013)259–265.

[14] T.R. Mahapatra, A.S. Gupta, Magnetohydrodynamics stagnation-point flow towards a stretching sheet, ActaMechanica 152 (2001) 191–196.

[15] A. Ishak, K. Jafar, R. Nazar, I. Pop, MHD stagnation point flow towards a stretching sheet, Physica A 388 (2009) 3377–3383.

[16] T.R. Mahapatra, S.K. Nandy, A.S. Gupta, Magnetohydrodynamic stagnation point flow of a power-law fluid towards a stretching sheet, Int. J. Non-LinearMech. 44 (2009) 124–129.

[17] A. Ishak, N. Bachok, R. Nazar, I. Pop, MHD mixed convection flow near the stagnation-point on a vertical permeable surface, Physica A 389 (2010) 40–46.

[18] Gangadhar, K., and Bhaskar Reddy, N., Chemically Reacting MHD Boundary Layer Flow of Heat and Mass Transfer over a Moving Vertical Plate in a Porous Medium with Suction, Journal of Applied Fluid Mechanics, Vol. 6, No. 1, pp. (2013)107-114.

[19] Able and Bataller R. C., Viscoelastic fluid flow and heat transfer over a

stretching sheet under the effects of a non-uniform heat source, viscous dissipation and thermal radiation. Int. J. Heat and Mass Transfer 50(15–16) (2007)3152–3162.

[20] Sandeep, N., Sulochana, C., & Kumar, R.., Flow and heat transfer in MHD dusty nanofluid past a stretching/shrinking surface with non-uniform source/sink. Walailak journal of Science and Technology, (2015)14(1).

[21] Sandeep, N., Sulochana, c., &Sugunamma, V.., Heat transfer characteristics of a dusty nanofluid past a permeable stretching/shrinking cylinder with non-uniform heat source/sink. Journal of Nanofluids, 5(1), (2016) 59-67.

[22] Ramana Reddy, J. V., Sandeep, N., Sugunamma, V., &Ananthakumar, K.,Influence of non uniform heat source/sink on MHD nanofluid flow past a slendering stretching sheetwith slip effects, Global Journal of Pure and Applied Mathematics, 12(1), (2016)247-254.

[23] El-Aziz, M. A., Viscous dissipation effect on mixed convection flow of a micropolar fluid over an exponentially stretching sheet, Can. J. Phys., Vol.87, (2009)pp.359-368.

[24] Sharma, R.,Ishak, A., Nazar, R., Pop, I., Boundary Layer Flow and Heat Transfer over a Permeable Exponentially Shrinking Sheet in the Presence of Thermal Radiation and Partial Slip, Journal of Applied Fluid Mechanics, Vol. 7, No. 1, pp. (2014)125-134.

[25] T.Prasannakumar and K.Gangadhar.,Slip flow of a casson fluid flow over an Exponentially Stretching Surface and Heat and Mass Transfer,International Research Journal of Engineering and Technology, vol.2 (2015) 56-72.